Effects of gas phase components on phosphorus removal from an iron-rich digested sludge

Sten Engblom, Viveka Öling-Wärnå and Nina Åkerback
Research, Development & Innovation, Novia University of Applied Sciences, Vasa, Finland
30.5.2022

EUROPEAN UNION
Interreg Botnia-Atlantica
European Regional Development Fund
region västerbotten
Region Västernorrland
Österbottens förbund Pohjanmaan liitto
YRKESHÖGSKOLAN NOVIA
SLU
HÄRNÖSAND ENERGI & MILJÖ
VAKIN
STORMOSSEN
BioFuel Region

CONTENT

ABSTRACT

Gas phase effects on key elements in digested sludge were investigated, with focus on phosphorus and its removal. Simplified models in the form of predominance diagrams were used to explore Eh-pH regions that are favourable to the precipitation of struvite or vivianite. Experiments performed included subjecting the digestate to conditions low in carbon dioxide and/or oxygen. Effects on key elements in the liquid phase of the digestate were in line with expectations and the simplified models.

KEYWORDS

Carbon dioxide, digestate, nutrient recovery, predominance diagrams, struvite, vivianite

HIGHLIGHTS

- Gas-phase levels of carbon dioxide and oxygen are important in effects exerted on digestate solution chemistry
- Predominance diagrams are used to map out Eh-pH regions where different phosphorus species dominate
- Effects of gas purging and dosing of magnesium are explored in laboratory-scale experiments

INTRODUCTION

The realization that phosphorus is a finite resource has initiated a flurry of research activities into recovery techniques for phosphorus-rich wastes and waste streams during the last decades (for an overview see e.g. Ohtake & Tsuneda 2019).

Struvite ($MgNH_4PO_4 \cdot 6H_2O$) has been a popular precipitate as it also removes nitrogen from solution (for a recent review see Li et al. 2019). The precipitation of struvite is also the basis of several techniques already in full-scale use. One such installation has recently been comprehensively reviewed (Saerens et al. 2021). In wastewater treatment plants, it has been the increased use of biological phosphorus removal that has furthered the use of phosphorus recovery as struvite (Britton et al. 2005).

On the other hand, it has been shown that when fermenting sludge from a wastewater treatment plant where iron is used as a coagulant in the waste water treatment process, a major part of the phosphate will form vivianite ($Fe(II)_3(PO_4)_2 \cdot 8H_2O$) with ferrous iron (Wilfert et al. 2018).

The effect of the carbonate system on the precipitation of struvite in digestate from a biogas reactor has been considered by many authors (e.g. Loewenthal et al. 1994; Stumpf et al. 2008; Korchef et al. 2011; Jordaan et al. 2013), mainly as a means to raise the pH value and thus initiate struvite precipitation by stripping of CO_2.

In this study Eh-pH diagrams and experiments have been used to investigate whether the presence or absence of CO_2 and/or O_2 can be used to promote the precipitation of either struvite or vivianite from an iron-rich digestate of sludge.

METHODS

Laboratory experiments

Fresh digestate directly from the sludge digestion reactor at the municipal waste management company Stormossen in Kvevlax, Finland, was collected in a plastic container that was immediately capped. The sludge comes from the wastewater treatment plant of the city of Vaasa, Finland, where both ferric sulfate and polyaluminium chloride are used in the process. The digestate was hygienised at 75 °C overnight while being semi-sealed in order to restrict oxygen from entering the container while allowing excess gas to escape.

After the digestate had cooled to room temperature its solid fraction was distributed homogeneously in the liquid by continuous stirring. The container was still being kept sealed to avoid letting in oxygen. The initial pH of the digestate was 8.58 and no pH adjustment was initially undertaken.

A peristaltic pump was used to extract a sample of the digestate. The sample´s solid phase was removed by centrifuging for 1 hour at 12000 $\times$ *g*. The supernatant was filtered through a 1.2 µm Minisart syringe filter (Sartorius) and sent to Hortilab (Närpes, Finland) where it was further filtered through a 0.45 µm filter and analysed by ICP-OES. Results are given as the start values in Table 1.

The peristaltic pump was then used to weigh 400 g portions of digestate into nine 0.5 litre bottles that were capped immediately.

The P content in the liquid phase of the original digestate was only 13 mg L^{-1} (Table 1). This is quite low and does not take into account any bound/adsorbed phosphate in the solid phase. It was estimated that 50 mg L^{-1} P in total was available for reaction. This equals $1.61 \cdot 10^{-3}$ M. An excess of Mg is usually recommended (Britton et al. 2005), and in this work the target Mg addition in concentration was set to $1.2 \times 1.61 \cdot 10^{-3}$ M = $1.94 \cdot 10^{-3}$ M, or 47.1 mg L^{-1}. The volume was approximately 0.4 L, and the Mg addition required was thus $0.774 \cdot 10^{-3}$ mol. This corresponds to 0.157 g $MgCl_2 \cdot 6H_2O$, which was added to each bottle.

The agitation system (bottle caps, motors and stir rods) of an AMPTS II system (BPC Instruments AB, Lund, Sweden) was used to provide stirring in the bottles, as well as gas inlets and outlets.

Utilizing the flow cell array/gas volume measuring device of the AMPTS II, three bottles were kept sealed and only excess gas was let out (bottles 3, 5 and 6; denoted Biogas in Table 1). Three bottles were aerated using a miniature diaphragm air pump (Gast 10D1125-101-1052) to bubble air through the digestate (bottles 7, 8 and 9; denoted Air in Table 1). Three bottles were purged with nitrogen gas by letting N_2 gas (99.997 % purity) from a cylinder bubble through the digestate (bottles 1, 2 and 4; denoted N_2 in Table 1).

The experiment lasted 10 days. All bottles were stirred throughout the experiment. During the first two days there was no gas purging. During days 3 and 4, purging with air/nitrogen was done during 8 hours per day. On day 5, pH adjustments were done. In the sealed bottles, with only excess gas being let out, the pH had decreased to about 8.3. In the six bottles with gas purging, the pH had decreased slightly to about 8.5. All bottles were adjusted to pH 8.7. All liquid levels that had decreased during the gas purging were restored using ultrapure (> 18.2 MΩ cm) water. During days 6 and 7, gas purging with air/nitrogen was continued for 8 hours per day. No purging took place on days 8 and 9, and the experiment was ended on day 10. Again, all liquid levels that had decreased were restored.

Measurements of pH and ORP (oxidation-reduction potential) were done immediately as described below.

Three Falcon tubes were filled from each bottle and centrifuged for one hour at 12000 $\times$ *g*. The supernatants from the three tubes were decanted into two tubes, and the tubes were again centrifuged for 45 minutes. The supernatants from the two tubes were pooled and filtered through a 1.2 µm Minisart syringe filter

(Sartorius). After acidification with 0.4 ml suprapur 65 % HNO_3 (Merck) to 40 ml sample, the samples were sent for ICP-OES analysis at Hortilab (Närpes, Finland) where they were further filtered through a 0.45 µm filter prior to analysis. A separate non-acidified sample was filtered through a 0.45 µm Filtropur S syringe filter (Sarstedt) and sent to the same lab for N analysis using a modified Kjeldahl method. Results are shown in Table 1.

The experiments were performed at an ambient laboratory temperature of 20 °C.

The solid phases from the centrifugations were collected and analysed by ICP-OES after drying and decomposition as described below.

Table 1. Measured total concentrations of selected elements in the liquid phase at the start and the end of the experiments, with mean values and standard deviations (SD).

Bottle	Gas phase	Al mg L^{-1}	Fe mg L^{-1}	Mg mg L^{-1}	Ca mg L^{-1}	P mg L^{-1}	S mg L^{-1}	N mg L^{-1}	pH	ORP mV	Eh mV
Start	Biogas	1.2	7.7	6.8	14	13	24	n.a.	8.58	n.a.	n.a.
1	N_2	15	58	6.8	33	36	18	2880	8.93	-442	-234
2	N_2	16	60	8.8	32	35	18	2640	8.84	-444	-236
4	N_2	14	58	11	31	32	15	2680	8.77	-429	-221
Mean	N_2	15	59	8.9	32	34	17	2730	8.84	-438	-230
SD	N_2	1.0	1.2	2.1	1.0	2.1	1.7	129	0.08	8.14	8.14
7	Air	1.6	20	21	23	21	26	2710	8.35	-365	-157
8	Air	2.4	23	18	22	19	43	2550	8.58	-432	-224
9	Air	2.1	23	19	23	17	210	2540	8.44	-363	-155
Mean	Air	2.0	22	19	23	19	93	2600	8.45	-387	-179
SD	Air	0.4	1.7	1.5	0.6	2.0	102	95.4	0.12	39.3	39.3
3	Biogas	4.0	24	16	26	21	18	2930	8.60	-425	-217
5	Biogas	4.2	21	15	22	31	19	2940	8.72	-362	-154
6	Biogas	4.0	22	18	23	27	19	2930	8.56	-354	-146
Mean	Biogas	4.1	22	16	24	26	19	2930	8.62	-380	-172
SD	Biogas	0.1	1.5	1.5	2.1	5.0	0.6	5.77	0.08	38.9	38.9

Analysis of solids

The solids from the centrifugation were dried overnight at 105 °C. After a thorough grinding and homogenization using an agate pestle and mortar, the powdered samples were sent to Hortilab for microwave assisted acid (HNO_3) digestion according to EPA 3051A and ICP-OES analysis.

Loss on ignition (LOI) was measured according to European Standard EN 12879. The results are presented in Table 2.

Table 2. Measured total concentrations of selected elements in the dry solid phase at the start and the end of the experiments, with mean values and standard deviations (SD).

Bottle	Gas phase	Al	Fe	Mg	Ca	P	S	LOI
		g kg^{-1}	g kg^{-1}	g kg^{-1}	g kg^{-1}	g kg^{-1}	g kg^{-1}	%
Start	Biogas	17.0	114	5.93	34.6	28.1	12.3	53.8
1	N_2	18.2	121	7.16	34.8	29.0	13.2	50.9
2	N_2	17.6	120	7.40	36.5	28.9	12.7	51.3
4	N_2	17.8	120	7.47	36.5	28.5	12.9	50.9
Mean	N_2	17.9	120	7.34	35.9	28.8	12.9	51.0
SD	N_2	0.31	0.58	0.16	0.98	0.26	0.25	0.23
7	Air	17.3	115	7.19	36.4	28.7	12.3	51.1
8	Air	17.6	116	7.42	37.3	28.4	9.73	51.2
9	Air	17.6	120	7.50	37.9	29.1	8.19	51.3
Mean	Air	17.5	117	7.37	37.2	28.7	10.1	51.2
SD	Air	0.17	2.65	0.16	0.75	0.35	2.08	0.10
3	Biogas	17.6	119	7.19	36.2	28.3	12.2	51.6
5	Biogas	17.5	116	7.49	37.1	28.0	12.4	51.3
6	Biogas	17.4	116	7.28	36.6	28.8	12.7	51.3
Mean	Biogas	17.5	117	7.32	36.6	28.4	12.4	51.4
SD	Biogas	0.10	1.73	0.15	0.45	0.40	0.25	0.17

ORP and pH measurements

The pH values were measured using a Hamilton FlaTrode electrode. ORP values were measured using a Hamilton ORP electrode. The ORP readings were drifting towards more negative potentials and values were taken when the drift was less than 1 mV/30 sec. These values were measured with respect to the built-in reference electrode and are therefore specific to the electrode used. For comparisons it is better to use Eh, which is the potential with respect to the standard hydrogen electrode (SHE). In order to convert ORP measurements to Eh values, the potential of the built-in reference electrode versus SHE has to be determined.

$$Eh = ORP_{measured} + E_{ref} \text{ vs SHE} \quad (1)$$

In this work E_{ref} vs SHE was determined according to Nordstrom (1977). The ORP value in ZoBell's solution (ZoBell 1948) is first measured. With the electrode used in this work it was found that

$$ORP_{ZoBell} = 234.4\ mV \quad (2)$$

According to Nordstrom (1977),

$$Eh_{ZoBell} = 0.43028 - 2.5157 \times 10^{-3}\ (t - 25) - 3.7979\ 10\ (t - 25)^2$$

$$= 0.44276\ V = 442.76\ mV\ at\ 20\ °C \quad (3)$$

where t is the temperature in degrees Celsius. Therefore

$$E_{ref}\ vs\ SHE = Eh_{ZoBell} - ORP_{ZoBell} = 442.76\ mV - 234.4\ mV = 208.36\ mV\ at\ 20\ °C \quad (4)$$

By adding this number to the measured ORP values, a conversion to Eh was achieved.

Predominance diagrams

Eh-pH predominance diagrams were drawn using the PhreePlot software (http://www.phreeplot.org/). This software contains an embedded version 3 of the PHREEQC software (Parkhurst & Appelo 2013). Equilibrium constants used were those provided in the wateq4f database supplied with the PhreePlot software, except for schwertmannite and struvite.

For schwertmannite the log K value of 18.0 (Bigham et al. 1996) was used for the solubility of the mean composition given by

$$Fe_8O_8(OH)_{4.8}(SO4)_{1.6} + 20.8H^+ \rightarrow 8Fe^{3+} + 1.6SO_4^{2-} + 12.8H_2O \quad (5)$$

For struvite the log K value of -13.69 (Bhuiyan et al. 2007) was used for the solubility of

$$MgNH_4PO_4 \cdot 6H_2O = Mg^{2+} + NH_4^+ + PO_4^{3-} + 6H_2O \quad (6)$$

A species dominates within the boundaries of its field of predominance, but neighbouring species can still exist and the closer one gets to a boundary the more of the other species will appear.

The diagrams represent systems in equilibrium. Three different cases with respect to the partial pressure of CO_2 were considered. In all cases, diagrams for Fe, P and Mg were drawn (Fig. 1). Regarding iron, pyrite was not allowed since its field of predominance completely covers corresponding fields for monosulfides. The monosulfides of iron such as greigite and mackinawite form first and are responsible for the characteristic black colour (Appelo & Postma 2005). For modelling the solution chemistry, mean concentrations of the measured parameters in the triplicates at the end of the experiment were used (Table 1).

The three CO_2 cases used were:

- N_2. This represents a system where a cooled and degassed digestate has been purged with nitrogen gas to remove as much as possible of the carbonate system as well as oxygen. The CO_2 partial pressure was set to 10^{-10} atm.
- Air. With the aerated digestate, the CO_2 concentration in the gas phase at the time of the experiments was taken as 410 ppm as a mole fraction (Global Monitoring Laboratory 2022), i.e. the partial pressure of CO_2 was 0.000410 atm.
- Biogas. As a worst-case scenario, a CO_2 partial pressure of 0.39 atm. was assumed. This is the mean CO_2 concentration in biogas from the Stormossen digestion of sludge. After the digestate is removed from the digester both cooling and degassing is taking place, so this value approximates a digestate as it emerges from the digestor.

Measured Eh-pH values (Table 1) are shown in the predominance diagrams as black dots.

Due to lack of information regarding the nature of the organic material present in the digestate, interactions with organic ligands and/or adsorbents is not taken into account in the diagrams. The diagrams are therefore intended for a qualitative guidance only because of the estimates involved, as well as the uncertainties in and lack of structural and thermodynamic information.

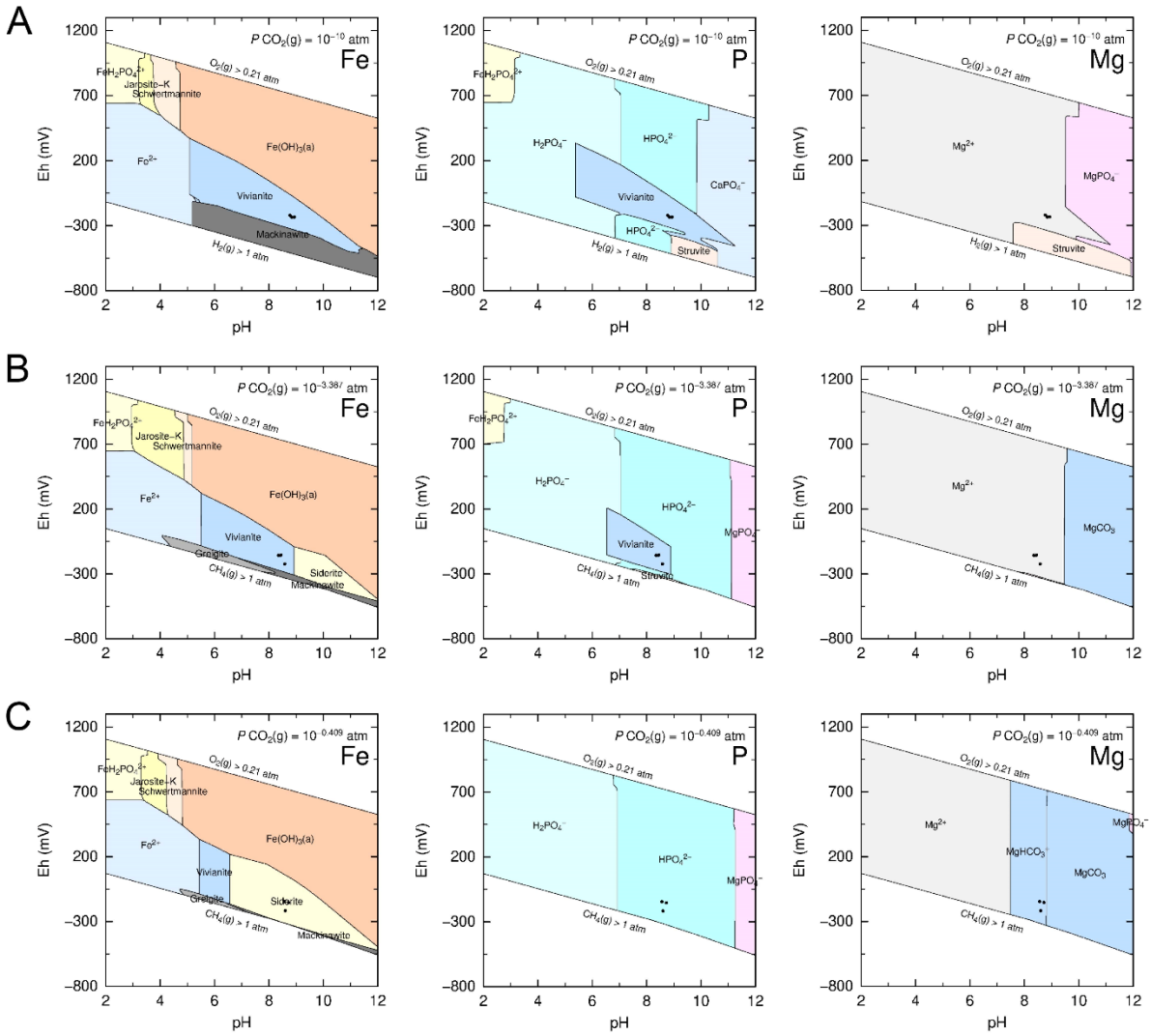

Figure 1. Eh-pH predominance diagrams for A: the N_2 cases, B: the Air cases, and C: the Biogas cases. Black dots indicate the experiments using the pH and Eh values from Table 1.

Statistical analysis

An ANOVA test was used when comparing the difference of Al, Fe, Mg, Ca, P, and N content in the liquid phase for the three different conditions. Statistically significant differences ($p < 0.05$) between the three cases in Table 1 (N_2, Air and Biogas) were found for all elements except for sulfur where the test yielded no statistically significant difference between the cases. The p values found were 5.1×10^{-7} (Al), 1.2×10^{-7} (Fe), 0.0008 (Mg), 0.0003 (Ca), 0.0041 (P), and 0.0127 (N). For p values lower than 0.05, a Tukey HSD (honestly significant differences) post hoc test was performed to identify which pair of conditions were significantly different from each other. Microsoft 365 Excel (version 2112) was used for ANOVA and the online web statistical calculator astatsa.com (https://astatsa.com/) was used for Tukey HSD test. Column charts with added p values were done for each of the elements in Excel. (Fig. 2).

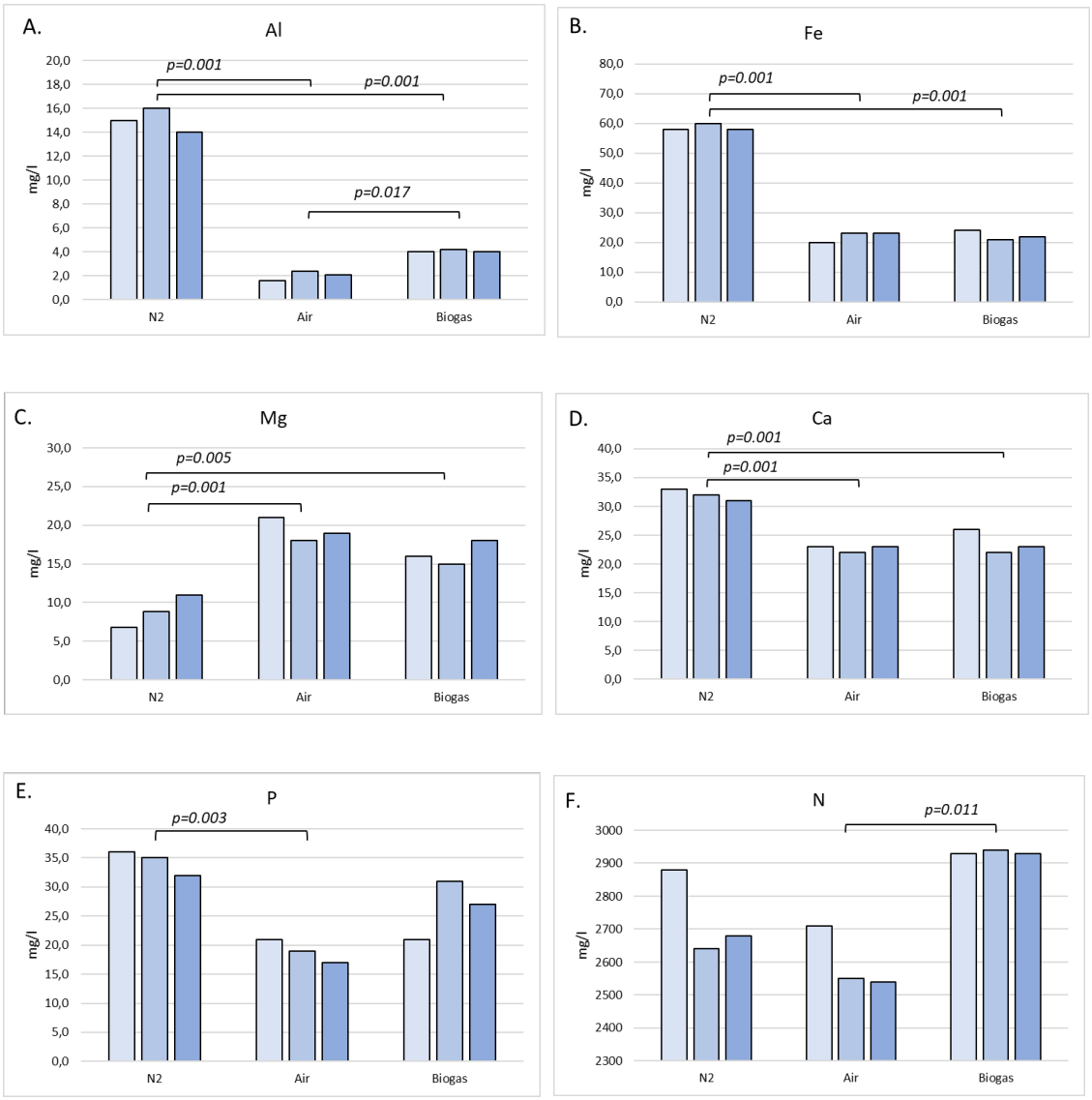

Figure 2. Total concentrations of selected elements (A-F) in the liquid phase for N_2 cases, Air cases and Biogas cases at the end of the experiments. (P values derived from the post-hoc Tukey HSD test for the different treatment pairs.)

RESULTS AND DISCUSSION

A digestate is a complex system involving both inorganic and organic components, defined by its solid, liquid and gas phases. Both pH and redox conditions will determine which species will dominate in certain situations.

In this work, no attempt was made to maximize the amount of phosphorus precipitated. Instead, the near-equilibrium concentrations of different analytes in both the liquid and the solid phases were explored, as a result of different O_2 and CO_2 levels in the gas phase.

The model used to create the Eh-pH diagrams is restricted to inorganic chemistry, and the influence of the organic matter is thus not taken into account due to lack of structural and thermodynamic information. This limits the usefulness of the models, but there is still enough agreement with changes in the concentrations measured in the liquid phase, and to some extent in the solid phase, to consider them to be of value as guidance.

Case N_2: Low CO_2, low O_2

As oxygen is removed by purging the solution with nitrogen gas (experiments denoted N_2 in Tables 1 and 2; Eh-pH diagrams in Fig. 1 A), the redox potential of the solution is pushed towards more reductive conditions, i.e., the activity of electrons is increased. In this work purging with N_2 lowered the redox potential by about 50 mV (Table 1) in comparison with the other experimental cases.

CO_2 is also removed which results in decreasing carbonate levels in the liquid phase as the reactions below are pushed to the right:

$$H^+ + CO_3^{2-} \leftrightarrow HCO_3^- + H^+ \leftrightarrow H_2CO_3 \leftrightarrow CO_2 (\uparrow) + H_2O \quad (7)$$

The prevalent reason for purging CO_2 is to increase the pH value as hydrogen ions are consumed in the process. However, the availability of magnesium will also be enhanced as carbonate levels are reduced. This will aid the formation of struvite as the competition in the form of magnesium bicarbonate and magnesium carbonate is suppressed (Fig. 1).

Purging with N_2 also removes CO_2 as a carbon source and electron acceptor in methane formation. According to the simplified models in Fig. 1, this would allow for more negative redox potentials to be reached. In the case of iron-rich digestates, the consequence would be that Eh-pH conditions that would favour struvite formation are in principle reachable. The reason for the rather modest lowering of the redox potential in the experiments is most likely the presence of other electron acceptors than oxygen. Ferric iron is one possibility (see the discussion in connection with Eqs 9 and 10 below), and sulfate is another candidate (see Eq. 11 below). The supply of electron acceptors has to be exhausted before the redox potential can be further lowered.

According to Table 1, the N_2 cases show an increase in both total Fe and P in the liquid phase. There are several possible sources for this. The equilibrium between struvite and vivianite

$$MgNH_4PO_4{\cdot}6H_2O + PO_4^{3-} + 2H_2O + 3Fe^{2+} \leftrightarrow Fe(II)_3(PO_4)_2{\cdot}8H_2O + Mg^{2+} + NH_4^+ \quad (8)$$

may be pushed to the left, i.e. towards struvite, as Eh-pH conditions indirectly become increasingly favourable for struvite formation through the precipitation of ferrous iron as a sulfide.

Also, in a continuously fed biogas reactor there may not be enough time to reduce all iron hydroxides during the digestion, so in the N_2 case the reduction of remaining ferric hydroxide is a possible source for the increase in Fe seen:

$$Fe(OH)_3 + e^- + 3H^+ \leftrightarrow Fe^{2+} + 3H_2O \quad (9)$$

Hydrogen ions is consumed in this process, contributing to a higher pH. Adsorbates on flocs of iron hydroxide would be released in this process. Also, an increased activity of electrons can dissolve the iron(III) phosphate as the ferric iron is reduced and Eq. 10 is pushed to the right:

$$Fe(III)PO_4 + e^- \leftrightarrow Fe^{2+} + PO_4^{3-} \quad (10)$$

If these processes occur, more and more ferrous iron and phosphate will be added to the solution. This would push the equilibrium in Eq. 8 to the right, i.e., towards the formation of vivianite, unless hindered by other circumstances/actions.

The addition of magnesium is such an action which would push Eq. 8 to the left. The relatively low Mg content for the N_2 cases in Table 1 indicate that at least some struvite formation is indeed taking place. According to Fig. 1 A only limited amounts of struvite will form as the Eh-pH conditions still are some way off optimal conditions for struvite formation. The liquid phase has a relatively high P content and a relatively

low Mg content in the N_2 cases, and an increased Mg addition in these experiments could have promoted increased struvite formation (Fig. 2C and 2E).

The relatively high Mg content in the solid phase could indicate struvite formation, but the Mg content of the solid phase is high in all experiments (Table 2). At present it is not possible to say if or how the Mg species in the solid phases of the different experiments differ or whether interactions with the organic material are important.

If the digestate is rich in sulfur, the formation of sulfide is also of interest. The Eh-pH diagram (Fig. 1 A) and the sulfur concentrations in Tables 1 and 2 indicate that we have some reduction of sulfate:

$$SO_4^{2-} + 8e^- + 4H^+ \leftrightarrow S^{2-} + 2H_2O \qquad (11)$$

This will promote the formation of black monosulfides such as mackinawite:

$$Fe^{2+} + S^{2-} \leftrightarrow Fe(II)S \qquad (12)$$

The digestates were also notably black after purging with N_2, as compared to the other experiments. Iron(II) being lost to sulfide formation will promote a push to the left of Eq. 8, i.e., struvite formation. The high iron content in the N_2 cases in Table 1 (and Fig. 2B) indicates that there may be grounds for adding sulfur to the digestate if one wishes to precipitate ferrous iron as a sulfide and thus promote struvite formation.

Aluminium will be present as both $AlPO_4$ and aluminium hydroxide flocs in the sludge (Yeoman et al. 1988). Purging with N_2 results in significantly increased Al concentrations (Table 1, Fig. 2A). Aluminium isn't a redox active metal such as iron, but the somewhat higher pH in this case (Table 1) could lead to increased dissolution of aluminium hydroxide flocs and/or aluminium phosphate and the formation of soluble $Al(OH)_4^-$.

Case Air: Atmospheric CO_2 and O_2 levels

When a digestate is aerated (experiments denoted Air in Tables 1 and 2; Eh-pH diagrams in Fig. 1 B; Fig. 2) we get a situation where the gas phase contains a stable O_2 level of 21 % by volume and a CO_2 level around 410 ppm by volume.

Oxygen will mop up electrons, but enough electron donors are still available to keep the redox potential low (Table 1). Vivianite is according to the model the dominating species both regarding iron and phosphorus (Fig. 1 B) and thus a sink for both iron and phosphate. Reactions in Eqs 9 and 10 are still of interest, if ferric iron still is available, as the redox potential is low enough for the reduction of ferric iron and the formation of vivianite pushes the reactions to the right. The sulfur content of the liquid phase is relatively high while the S content in the solid phase is reduced, indicating favourable conditions for the sulfate species.

The magnesium content in the liquid phase is higher in these cases (Fig. 2C), which supports the indication that struvite is not formed to any larger extent. The relatively high Mg content in the solid phases follows the results of the other experiments and indicates an immobilization in the solid phase.

The pH is lower than in the N_2 and Biogas cases. Aeration should reduce carbonate levels and actually raise the pH as hydrogen ions are consumed as the reactions in Eq. 7 are pushed to the right. The lowering of the pH indicates that some other process adds hydrogens ions, and one possible candidate is the oxidation of sulfide, Eq. 11.

Case Biogas: High CO_2, low O_2

A digestate in equilibrium with a gas phase consisting of biogas (experiments denoted Biogas in Tables 1 and 2; Eh-pH diagrams in Fig. 1 C; Fig. 2) resembles the situation in the digestor except that the digestate is cooling and no longer maintaining a temperature ideal for fermentation.

Ferrous iron is now likely to predominantly form $Fe(II)CO_3$ or siderite (Fig. 1), which will serve as a sink for both iron and carbonate. A carbonate sink would contribute to a lowering of the pH, and the pH in the sealed bottles did decrease the most prior to the pH adjustment (see the Experimental section). Magnesium carbonate is also a possible carbonate sink.

Neither vivianite nor struvite is likely to form according to the model used in this work (Fig. 1). If ferric iron is still available after the digestion, it may contribute to the iron and phosphorus content of the liquid phase through Eqs 9 and 10 as the redox potential is low enough for the ferrous form to dominate.

There may be some magnesium in the precipitate in the form of carbonate. Otherwise, as discussed below, the solid phases are remarkably similar in all cases with respect to the total concentrations of the components measured in this work.

The higher nitrogen content in this case (Table 1; Fig. 2) is likely a consequence of the sealed bottles. Nitrogen losses in the form of ammonia are likely in the cases with N_2 or air purging.

The solid phase

There is remarkably little variation between experiments in the total concentrations of the measured analytes in the solid phase (Table 2). However, the changes that can be noted are in line with changes in the Eh-pH diagrams (Fig. 1). E.g., the S content is increased slightly (+4.9 %) compared to the start value in the N_2 case, where an increase in precipitated S as sulfide is expected. Aeration yields a reduction ($-$17.9 %) compared to the start value in precipitated S as the soluble sulfate form is expected to dominate.

Regarding magnesium, there is a notable increase (about +24 %) compared to the start value in the Mg content in the solid phases but this increase is the same irrespective of experiment. This may not be a function of the chemistry explored in the Eh-pH diagrams but could be, e.g., an indication of magnesium's association with the organic matter in the solid phase. For a discussion on the effect of organic matter on struvite formation, see Muhmood et al. (2021).

In this work it has not been possible to determine the different precipitated species in the solid phase, and thus not possible to resolve how the biogas digestion and the post-digestion equilibration with different gas phases affected different precipitated species and the extent of their dissolution and reprecipitation. Loss on ignition follows the other measured parameters and is thus remarkably similar in all cases (Table 2).

CONCLUSIONS

If CO_2 and O_2 are purged, the Eh-pH diagram indicates a window at reducing redox potentials where struvite will be the dominating phosphorus species even in the presence of iron. However, in the experiments in this work the purging with N_2 did not push the redox potential far enough. The reason is most likely the remaining presence of other electron acceptors than oxygen. The phosphorus precipitate in the experiments in this work was most likely a mixture of vivianite and struvite. In addition, dosing of both magnesium and sulfur is probably required in order to further promote struvite formation and to mask ferrous iron. If an Eh-pH region where struvite dominates is reachable can only be determined in future work.

Aeration favours vivianite formation. Even though a steady supply of oxygen is provided, there are enough electron donors in the digestate to maintain a low redox potential. According to the model used, the carbonate levels are low enough to let vivianite be the dominating iron species, in contrast to the high CO_2 case where siderite dominates at pH values normally encountered in digestates.

The worst-case scenario is the high CO_2, low O_2 case where the digestate is in equilibrium with a gas phase consisting of biogas. No solid phosphorus phase dominates according to the model used in this work. Ferrous iron is more likely to occur as siderite and magnesium is mainly associated with bicarbonate and carbonate.

Organic matter in the form of ligands and adsorbents was not taken into account in the models used to create the predominance diagrams. This limits the value of the models, but changes in the gas phase induce changes in the measured concentrations in the liquid phase, and to some extent also in the solid phase, that still agree qualitatively with changes indicated by the models.

With the notable exception of sulfur, the total concentrations of the measured elements in the solid phases remained largely the same in all experiments.

ACKNOWLEDGEMENTS

This study was part of the project Bothnia Nutrient Recycling funded by the European Regional Development Fund via the Interreg Botnia-Atlantica program. Co-funders of the project were the Regional Council of Ostrobothnia, Region Västerbotten, Region Västernorrland, Härnösand Energi & Miljö and VAKIN.

REFERENCES

Appelo C. A. J. & Postma D. 2005 *Geochemistry, groundwater and pollution*. 2nd edn, A.A. Balkema Publishers, Leiden, the Netherlands.

Bhuiyan M. I. H., Mavinic D. S. & Beckie R. D. 2007 A solubility and thermodynamic study of struvite. *Environmental Technology*, 28(9), 1015-1026. https://doi.org/10.1080/09593332808618857

Bigham J. M., Schwertmann U., Traina S. J., Winland R. L. & Wolf M. 1996 Schwertmannite and the chemical modelling of iron in acid sulfate waters. *Geochimica et Cosmochimica Acta*, 60(12), 2111-2121. https://doi.org/10.1016/0016-7037(96)00091-9

Britton A., Koch F. A., Mavinic D. S., Adnan A., Oldham W. K. & Udala B. 2005 Pilot-scale struvite recovery from an anaerobic digester supernatant at an enhanced biological phosphorus removal wastewater treatment plant. *Journal of Environmental Engineering and Science*, 4(4), 265-277. https://doi.org/10.1139/s04-059

Global Monitoring Laboratory 2022 Trends in atmospheric carbon dioxide. https://gml.noaa.gov/ccgg/trends/global.html (accessed 19 January 2022)

Jordaan E. M., Rezania B. & Çiçek N. 2013 Investigation of chemical-free nutrient removal and recovery from CO_2-rich wastewater. *Water Science & Technology*, 67(10), 2195-2201. https://doi.org/10.2166/wst.2013.116

Korchef A., Saidou H. & Ben Amor M. 2011 Phosphate recovery through struvite precipitation by CO_2 removal: Effect of magnesium, phosphate and ammonium concentrations. *Journal of Hazardous Materials*, 186(1), 602-613. https://doi.org/10.1016/j.jhazmat.2010.11.045

Li B., Boiarkina I., Yu W., Huang H. M., Munir T., Wang G. Q. & Young B. R. 2019 Phosphorus recovery through struvite crystallization: Challenges for future design. *Science of the Total Environment*, 648, 1244-1256. https://doi.org/10.1016/j.scitotenv.2018.07.166

Loewenthal R.E., Kornmüller U. R. C. & van Heerden E. P. 1994 Modelling struvite precipitation in anaerobic treatment systems. *Water Science & Technology*, 30(12), 107-116. https://doi.org/10.2166/wst.1994.0592

Muhmood A., Wang X., Dong R. & Wu S. 2021 New insights into interactions of organic substances in poultry slurry with struvite formation: An overestimated concern? *Science of the Total Environment*, 751, 141789. https://doi.org/10.1016/j.scitotenv.2020.141789

Nordstrom D. K. 1977 Thermochemical redox equilibria of ZoBell's solution. *Geochimica et Cosmochimica Acta*, 41(12), 1835-1841. https://doi.org/10.1016/0016-7037(77)90215-0

Ohtake H. & Tsuneda S. (eds) 2019 *Phosphorus Recovery and Recycling*. Springer, Singapore.

Parkhurst D. L. & Appelo C. A. J. 2013 Description of input and examples for PHREEQC version 3 – A computer program for speciation, batch-reaction, one-dimensional transport, and inverse geochemical calculations. In *U.S. Geological Survey Techniques and Methods*. Book 6, Chapter A43. https://pubs.usgs.gov/tm/06/a43/

Saerens B., Geerts S. & Weemans M. 2021 Phosphorus recovery as struvite from digested sludge – experience from the full scale. *Journal of Environmental Management*, 280, 111743. https://doi.org/10.1016/j.jenvman.2020.111743

Stumpf D., Zhu H., Heinzmann B. & Kraume M. 2008 Phosphorus recovery in aerated systems by MAP precipitation: optimizing operational conditions. *Water Science & Technology*, 58(10), 1977-1983. https://doi.org/10.2166/wst.2008.549

Wilfert P., Dugulan A. I., Goubitz K., Korving L., Witkamp G. J. & Van Loosdrecht M. C. M. 2018 Vivianite as the main phosphate mineral in digested sewage sludge and its role for phosphate recovery. *Water Research*, 144, 312-321. https://doi.org/10.1016/j.watres.2018.07.020

Yeoman S., Stephenson T., Lester J. N. & Perry R. 1988 The removal of phosphorus during wastewater treatment: A review. *Environmental Pollution*, 49(3), 183-233. https://doi.org/10.1016/0269-7491(88)90209-6

ZoBell C. E. 1946 Studies on redox potential of marine sediments. *Bulletin of the American Association of Petroleum Geologists*. 30(4), 477-513. https://doi.org/10.1306/3D933808-16B1-11D7-8645000102C1865D